Title	Interseismic pore compaction suppresses earthquake occurrence and causes faster apparent fault loading
Author(s)	Mitsui, Yuta; Hirahara, Kazuro
Citation	Geophysical Research Letters (2009), 36(20)
Issue Date	2009
URL	http://hdl.handle.net/2433/91536
Right	Copyright 2009 by the American Geophysical Union.
Type	Journal Article
Textversion	author

Interseismic pore compaction suppresses earthquake occurrence and causes faster apparent fault loading

Yuta Mitsui

Department of Geophysics, Graduate School of Science, Kyoto University, Kyoto, Japan

Kazuro Hirahara

Department of Geophysics, Graduate School of Science, Kyoto University, Kyoto, Japan

Physical and chemical processes operating on faults during interseismic periods are important for earthquake generation. In this study, we focus on pore compaction within fault zones driven by chemical kinetic effects. One established model of compaction causes an increase of pore fluid pressure almost linearly with time, if fluid diffusion is neglected. We introduced it into a simple numerical model for earthquake cycles and found that this effect can drastically change the recurrence of earthquakes: (1) It gradually stabilizes the fault and eventually suppresses earthquake occurrence (2) It surprisingly causes faster "apparent" fault loading. Furthermore, we developed an expression for the "apparent" loading velocity and checked that it is consistent with the results of numerical calculations. We also extended the expression for the "apparent" loading velocity to include the effect of pore dilatancy. This "apparent" loading would not only appear in a simple elastic system with a single degree of freedom, but also in complicated systems that involve simulations of realistic earthquake cycles.

1. Introduction

Since pore fluid may exist within fault zones (*Evans and Chester* [1995], among many others), effects of pore fluid on earthquake generation are worth to be investigated. Recently, we suggested that thermal pressurization of pore fluid, which notably operates during coseismic periods, can prolong earthquake recurrence intervals via increases of static stress drop (*Mitsui and Hirahara* [2009]). Now, in addition, we attempt to add the other perspective for earthquake generation. It is pore compaction within fault zones driven by chemical kinetic effects (hereinafter referred to as PCC) such as pressure solution crack sealing (e.g., *Gratier et al.* [2003]). This effect causes the gradual increase of pore fluid pressure over a long time which may be compared with interseismic periods of earthquake cycles.

PCC has been previously modeled by some studies. The recent one of them, *Gratier et al.* [2003], integrated some complicated components of kinetic reaction to present exponentially temporal decrease of porosity with one characteristic time and modeled the interseismic evolution of pore fluid pressure. This sophistication can be introduced easily into numerical models of earthquake cycles. Now, we set a precedent for performing it using a simple elastic system with a single degree of freedom.

2. Numerical Model

Our numerical system excluding the part of the evolution of pore pressure is the same as *Mitsui and Hirahara* [2009].

First of all, we assume a homogeneous fault patch in a uniform infinite elastic body. On the fault patch, spatially uniform relative slip is controlled by loading stress τ and frictional stress τ_f. Under assumptions of quasi-static balance of τ and τ_f accompanying energy lost through elastic wave radiation, $Gv/2c_s$, the relation between τ, τ_f and the slip velocity v is governed by:

$$v = [\tau - \tau_f]\frac{2c_s}{G} \tag{1}$$

where c_s is shear wave velocity and G is rigidity. Next, with elastic stiffness k, τ is driven by a far-field steady loading rate v_0 :

$$\tau = k[v_0 t - u] + \tau_0 \tag{2}$$

where t is time and u is the amount of total slip, and τ_0 is the initial loading stress balanced with the initial frictional stress at $t = u = 0$. The term $v_0 t - u$ is commonly called slip deficit. The degree of fault loading depends on that of slip deficit.

Subsequently, with regard to τ_f, it is generally divided into effective normal stress $\bar{\sigma}$ and the frictional coefficient μ. Under the condition that real contact area is sufficiently smaller than macroscopic contact area at a friction surface, effective normal stress $\bar{\sigma}$ is given by:

$$\frac{\tau_f}{\mu} = \bar{\sigma} = \sigma - p \tag{3}$$

where σ and p respectively denote normal stress and pore fluid pressure. Therefore, the increase of p by PCC causes the decrease of τ_f.

The formulation of PCC is rather simple following *Gratier et al.* [2003], although it includes complex processes of mineral dissolution (e.g., pressure solution), its diffusion by trapped fluid and its precipitation on pore surface. Porosity ϕ is assumed to decrease exponentially with time t:

$$\phi = \phi_0 \exp\left(\frac{-t}{X}\right) \tag{4}$$

where ϕ_0 is an initial value of the porosity and X is the characteristic time of PCC which depends on temperature, pore geometry and substance-specific constants for chemical reaction (*Renard et al.* [2000]). It is accompanied by the increase of the pore pressure p. If we distinguish between irreversible and elastic pore deformation and assume constant solid compressibility (*Segall and Rice* [1995]; *Gratier et al.* [2003]) and ignore fluid flow for simplicity, the evolution of p can be written as:

Table 1. Common parameters in this study.

Property	Symbol	Value	Units
Shear wave velocity	c_s	3500	m/s
Rigidity	G	34.3	GPa
Normal stress	σ	0.15	GPa
Reference pore pressure	p_0	0.14	GPa
Stiffness	k	1.25	MPa/m
Frictional coefficient	μ_0	0.6	
Friction parameter	a	0.01	
Friction parameter	b	0.015	
Friction parameter	L	0.02	m
Solid compressibility	β	1.0×10^{-9}	/Pa
Fluid compressibility	β_f	1.0×10^{-10}	/Pa
Porosity	ϕ	0.01	

$$\frac{dp}{dt} = -\frac{d\phi/dt}{\phi[\beta+\beta_f]} \simeq \frac{1}{[\beta+\beta_f]X} \tag{5}$$

where β is the compressibility of solid and β_f is that of pore fluid. This formula represents the linear increase of p with time.

In addition, regarding the frictional coefficient μ, in order to cause a stick-slip behavior, we use the laboratory-derived rate- and state-dependent law (*Dieterich* [1979]; *Ruina* [1980]):

$$\frac{\tau_f}{\bar{\sigma}} = \mu = \left[\mu_0 + b\ln\left(\frac{v_0\theta}{L}\right)\right] + a\ln\left(\frac{v}{v_0}\right) \tag{6}$$

where a is a governing parameter for the direct effect of velocity on friction, and b and L are the governing parameters for the friction evolution. As well known, two major evolution laws for θ exist. Because the difference of them is not a subject in this study, the most popular aging law (*Ruina* [1980]; based on *Dieterich* [1979])

$$\frac{d\theta}{dt} = 1 - \frac{v\theta}{L} \tag{7}$$

is assumed in this paper. But it is noteworthy that we tried assuming the other evolution law (*Ruina* [1983]) or the "Linker-Dieterich effect" (*Linker and Dieterich* [1992]) of normal stress alteration on the state evolution, and verified following characteristic results unchanging.

Common parameters used in this study are provided in Table 1. The values of these parameters are the same as those in *Mitsui and Hirahara* [2009] which are chosen as an example within possible ranges. The rest of the parameters are the characteristic time X and the loading velocity v_0. The former for a natural fault remains unknown, while *Gratier et al.* [2003, 2009] supposed it in the range of 1 day to 10^5 years. Thus, we change its value in a wide range and investigate its effects. In addition, we also change the value of v_0 for investigating effects of X.

For numerical calculations, we set an initial steady state condition as $v = 0.1v_0$, $\theta = L/[0.1v_0]$, $p = p_0$, $\phi = \phi_0$ and $\tau = \tau_f$. To solve the above constitutive relations, we first differentiate equations (1)-(4), (6) with respect to time and then integrate the coupled equations (1)-(7) by a Runge-Kutta method with adaptive step-size control (*Press et al.* [1992]).

3. Results

Our model calculations without PCC naturally exhibit a stick-slip like behavior at a constant frequency. In contrast, our calculations with PCC reveal different behaviors. Examples are shown in Figure 1.

One characteristic result in Figure 1 is that introduction of PCC causes to gradually suppress the stick-slip behavior and shorten the interseismic interval. Moreover, the shorter X causes the stronger effects. It is owing to the time decreases of the "critical fault stiffness" k_c (*Ruina* [1983]) via the time increases of p, where k_c is equal to $[\sigma-p][b-a]/L$ in quasi-static regimes. Since $k > k_{\rm crit}$ and $k < k_{\rm crit}$ respectively cause stable and unstable responses, the time decreases of k_c owing to PCC lead to stabilizing faults.

The other characteristic result in Figure 1, one may be surprised, is that introduction of PCC causes larger amount of slip until some point in time, which represents $\sigma \simeq p$. It means faster "apparent " loading than v_0 (30 mm/year in these cases). Moreover, the shorter X also causes the stronger effect.

We further investigate the PCC effect on the "apparent" loading. Figure 2 shows the values of the "apparent" loading velocity when we set several values of X and v_0, where we estimate the "apparent" loading velocity v_{ap} at the final (when $\sigma \simeq p$) slip amount divided by the final time from the initial condition, under the simple assumption of steady "apparent" loading. These results infer that the PCC effect with sufficiently small X obscures the real loading velocity v_0.

In order to interpret the notable effect of PCC on fault loading, we analyze the constitutive equations. If we substitute equations (2) and (3) into equation (1) and differentiate it with respect to t, we obtain $dv/dt = [2c_s/G][k[v_0 - v] - \bar{\sigma}d\mu/dt + \mu dp/dt]$. Then, neglecting dv/dt and $d\mu/dt$ which stand out only during coseismic periods (further the latter depends on the rate and state for cyclic behaviors), the constitutive relation becomes

$$k[v - v_0] \simeq \mu\frac{dp}{dt} \simeq \mu_0\frac{dp}{dt} \tag{8}$$

The approximation $\mu \simeq \mu_0$ can be approved practically. It means that the "apparent" loading velocity v_{ap} is

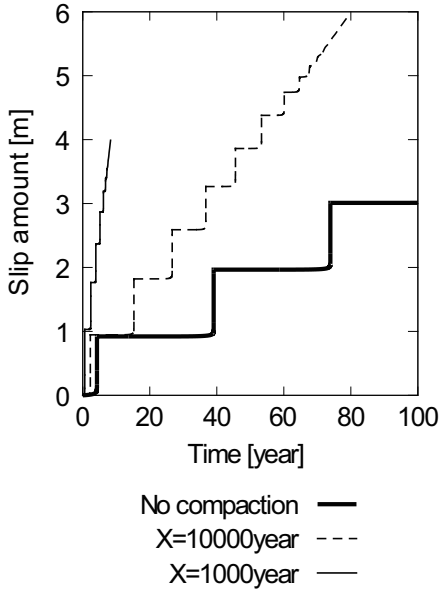

Figure 1. Examples of the calculated earthquake cycle where we set $v_0 = 30$ mm/year. The thick line indicates the case of no compaction, while the dotted and thin lines represent the cases of compaction with the characteristic time X of 10000 and 1000 years, respectively.

$$v_{ap} \simeq v_0 + \frac{\mu_0}{k}\frac{dp}{dt} = v_0 + \frac{\mu_0}{k[\beta+\beta_f]X} \tag{9}$$

In this formulation, v_{ap} does not depend on the level of effective normal stress, or porosity.

In Figure 2, we also shows the analytically calculated values of the "apparent" loading velocity using equation (9). They well correspond with the numerically calculated results.

4. Discussion

4.1. Is the "apparent" loading a general phenomenon?

If we would like to understand the above "apparent" loading intuitively, equations (1)-(3) can help us understand. With long-term steady effects for $dp/dt > 0$, namely $d\bar{\sigma}/dt < 0$, τ_f decreases steadily and τ also decreases following τ_f. In order to decrease τ, u should exceed $v_0 t$. Therefore $v_{ap} \simeq u/t$ has to unexpectedly exceed v_0 independently of details of the evolutions of frictional coefficient or pore pressure. Namely, from a viewpoint of the seismic coupling coefficient, which corresponds with coseismic slip amount divided by real loading, our results show that the coefficient exceeds 1 during initial unstable stick-slip regimes and decreases to 0 as $p \to \sigma$. Although we only perform the numerical calculations in the simple system with a single degree of freedom, the "apparent" loading would necessarily appear in rather complicated systems which assume the fault loading dependent on slip deficit. Possibly this is a phantom phenomenon, and it might be the next serious problem for numerical modelers.

4.2. Effects of pore dilatancy?

In the above simple calculations, we ignore possible effects of fluid flow and pore dilatancy. These effects may effectively restrain the PCC effects.

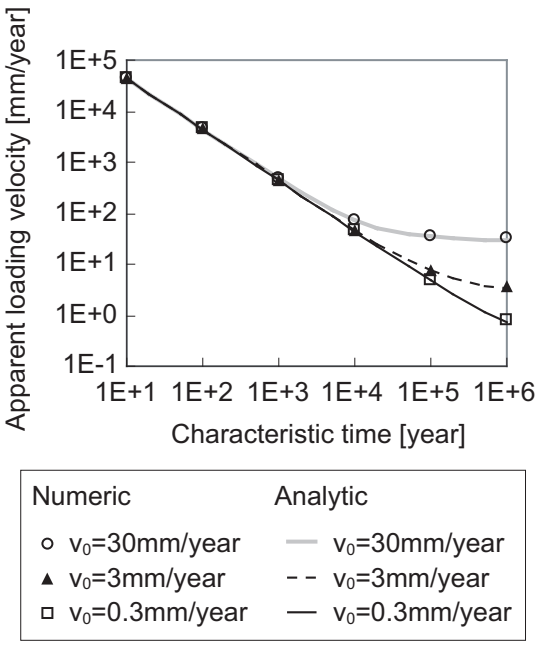

Figure 2. Results of the apparent loading velocity for several values of X and v_0. The markers represent the calculation results and the lines represent the analytic results using equation (9).

Especially, pore dilatancy has effects on pore pressure opposite to PCC. The combined effects of PCC and pore dilatancy should be considered for more realistic conditions. If we assume a simple velocity-dependent dilatancy (*Suzuki and Yamashita* [2007])

$$\left.\frac{d\phi}{dt}\right|_{dil} = Yv \tag{10}$$

Adding this effect alters the pore pressure evolution (equation (5)). Examples of the calculation results are shown in Figure 3. The introduction of the dilatancy decreases the pore pressure at each seismic event. It is notable that the dilatancy effectively restrains the seismic slip (this dilatancy hardening effect was previously shown by *Segall and Rice* [1995]) and the "apparent loading". In particular, when $t \ll X$, namely porosity does not pronouncedly decrease from its initial value, the time evolution of p is

$$\frac{dp}{dt} = -\frac{d\phi/dt}{\phi[\beta+\beta_f]} = \frac{-[-\phi_0 \exp(-t/X)/X + Yv]}{\phi[\beta+\beta_f]} \simeq \frac{1}{[\beta+\beta_f]X} - \frac{Yv}{\phi_0[\beta+\beta_f]} \tag{11}$$

Thus we obtain modified formulation of the "apparent" loading velocity v_{ap}

$$v_{ap} = \frac{v_0 + \mu_0/[k[\beta+\beta_f]X]}{1 + \mu_0 Y/[k[\beta+\beta_f]\phi_0]} \tag{12}$$

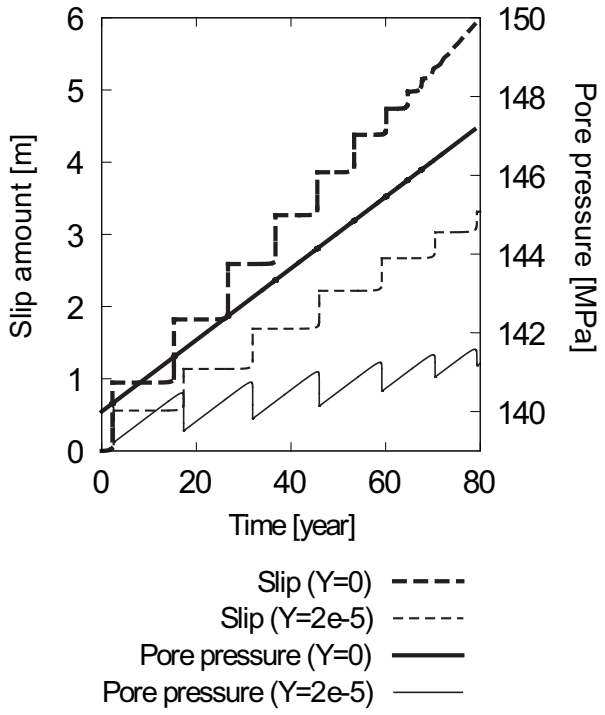

Figure 3. Examples of the calculated earthquake cycle where we set $X = 10000$ years and $v_0 = 30$ mm/year. The thick lines indicates the case of no dilatancy ($Y = 0$), while the thin lines do the case with the dilatancy effect ($Y = 2 \times 10^{-5}$). Moreover the dotted and solid lines represent the slip amount and the pore pressure, respectively.

If Y is sufficiently smaller than $k[\beta + \beta_f]\phi_0/\mu_0$, the dilatation effect can be ignored because equation (12) results in equation (9).

4.3. Does this model represent fault-valve behavior?

Sibson [1992] suggested that earthquake recurrences accompany fluid overpressurization during interseismic periods and release with earthquakes. Such the behavior was named "fault-valve behavior".

Our simple model including only the effects of PCC does not represent that concept. It can be called "fault pressurized behavior". However, it should be noted that the pore pressure evolution in the model with the pore dilatancy (shown in the previous section) denotes the same tendency of the fault-valve concept. In case of weak dilatancy, although the PCC effect for the apparent loading is moderated, it can certainly operate. This might be a new viewpoint on the fault-valve behavior. Furthermore, although our present model only represents the period until p reaches σ, there might be a larger-scale cycle including the process of hydrofracture with $p \sim \sigma$.

4.4. Experimental supports

Albeit the PCC effects are implied by field observations and theories, and confirmed in indentation experiments (*Gratier et al.* [2009]), and whether it operates effectively in real faults has not been confirmed yet.

But in laboratory sliding experiments, it was reported that the frictional resistance can be notably decreased by compaction (*Blanpied et al.* [1992]), although the spatiotemporal scales of loading for natural faults and laboratory experiments are rather different.

5. Conclusion

We introduced the effects of pore compaction within fault zones driven by chemical kinetic effects, into simple numerical model for earthquake cycles. The pore compaction results in earlier earthquake generation via faster "apparent" fault loading. However, it should be noted that the progression of pore compaction eventually suppresses the earthquake occurrence.

We developed an expression for the "apparent" loading velocity and checked that it is consistent with the results of numerical calculations. In addition, we developed a modified expression for the "apparent" loading velocity including the effect of pore dilatancy. Unexpectedly, this "apparent" loading would not only appear in a simple system with a single degree of freedom, but also in complicated systems that involve simulations of realistic earthquake cycles, as long as we assume fault loading depends on slip deficit.

Acknowledgments. We thank two anonymous reviewers and an associate editor. This research has been supported primarily by the Japan Society for the Promotion of Science (20-230) and a Grant-in-Aid for Scientific Research (B) (20340119) from MEXT.

References

Blanpied, M. L., D. A. Lockner, and J. D. Byerlee (1992), An earthquake mechanism based on rapid sealing of faults, *Nature*, *358*, 574–576.

Dieterich, J. H. (1979), Modeling of rock friction 1. Experimental results and constitutive equations, *J. Geophys. Res.*, *84*(B5), 2161–2168.

Evans, J. P., and F. M. Chester (1995), Fluid-rock interaction in faults of the San Andreas system: Inferences from San Gabriel fault rock geochemistry and microstructures, *J. Geophys. Res.*, *100*(B7), 13,007–13,020.

Gratier, J.-P., P. Favreau, and F. Renard (2003), Modeling fluid transfer along california faults when integrating pressure solution crack sealing and compaction processes, *J. Geophys. Res.*, *108*(B2), doi:10.1029/2001JB000380.

Gratier, J.-P., R. Guiguet, F. Renard, L. Jenatton, and D. Bernard (2009), A pressure solution creep law for quartz from indentation experiments, *J. Geophys. Res.*, *114*(B03403), doi:10.1029/2008JB005652.

Linker, M. F., and J. H. Dieterich (1992), Effects of variable normal stress on rock friction: Observations and constitutive equations, *J. Geophys. Res.*, *97*(B4), 4923–4940.

Mitsui, Y., and K. Hirahara (2009), Coseismic thermal pressurization can notably prolong earthquake recurrence intervals on weak rate and state friction faults: Numerical experiments using different constitutive equations, *J. Geophys. Res.*, *in press.*, doi:10.1029/2008JB006220.

Press, W. H., B. P. Teukolsky, and W. T. Vetterling (1992), *Numerical Recipes*, 2nd ed., Cambridge University Press, New York.

Renard, F., J.-P. Gratier, and B. Jamtveit (2000), Kinetics of crack-sealing, intergranular pressure solution, and compaction around active faults, *J. Struct. Geol.*, *22*, 1395–1407.

Ruina, A. (1980), Friction laws and instabilities: A quasistatic analysis of some dry frictional behavior, Ph.D. thesis, Cornell University.

Ruina, A. (1983), Slip instability and state variable friction laws, *J. Geophys. Res.*, *88*(B12), 10,359–10,370.

Segall, P., and J. R. Rice (1995), Dilatancy, compaction and slip instability of a fluid-infiltrated fault, *J. Geophys. Res.*, *100*(B11), 22,155–22,171.

Sibson, R. H. (1992), Implications of fault-valve behavior for rupture nucleation and recurrence, *Tectonophysics*, *211*, 283–293.

Suzuki, T., and T. Yamashita (2007), Understanding of slip-weakening and -strengthening in a single framework of modeling and its seismological implications, *Geophys. Res. Lett.*, *34*(L13303), doi:10.1029/2007GL030260.

Yuta Mitsui
Department of Geophysics, Graduate School of Science, Kyoto University, Kitashirakawa-Oiwakecho, Sakyo, Kyoto 606-8224, Japan (mitsui@kugi.kyoto-u.ac.jp)